MASTER COPY KEEP THIS COPY FOR REPRODUCTION PURPOSES

(1)

AD-A247 528

1. AGENCY USE ONLY (Leave blank)	2. REPORT DATE	3. REPORT TYPE AND DATES COVERED
	January 16, 1992	

4. TITLE AND SUBTITLE Monte Carlo Simulations of Random Rough Surface Scattering with Finite Element and Finite Difference Methods

5. FUNDING NUMBERS

6. AUTHOR(S)

Leung Tsang And Chi Hou Chan

7. PERFORMING ORGANIZATION NAME(S) AND ADDRESS(ES)

University of Washington
Seattle, WA 98195

8. PERFORMING ORGANIZATION REPORT NUMBER

9. SPONSORING/MONITORING AGENCY NAME(S) AND ADDRESS(ES)

U. S. Army Research Office
P. O. Box 12211
Research Triangle Park, NC 27709-2211

10. SPONSORING/MONITORING AGENCY REPORT NUMBER

11. SUPPLEMENTARY NOTES

The view, opinions and/or findings contained in this report are those of the author(s) and should not be construed as an official Department of the Army position, policy, or decision, unless so designated by other documentation.

12a. DISTRIBUTION/AVAILABILITY STATEMENT

Approved for public release; distribution unlimited.

12b. DISTRIBUTION CODE

13. ABSTRACT *(Maximum 200 words)*

Monte Carlo simulations of scattering of waves by one-dimensional random rough gold surfaces at optical frequencies are investigated by the use of the finite-element method. Both TE and TM plane wave incidences are considered. Backscattering enhancements are observed for all the cases studied in this report.

14. SUBJECT TERMS	15. NUMBER OF PAGES
Random rough surface, Monte Carlo simulations, backscattering enhancement, finite-element method	4
	16. PRICE CODE

17. SECURITY CLASSIFICATION OF REPORT	18. SECURITY CLASSIFICATION OF THIS PAGE	19. SECURITY CLASSIFICATION OF ABSTRACT	20. LIMITATION OF ABSTRACT
UNCLASSIFIED	UNCLASSIFIED	UNCLASSIFIED	UL

FINAL REPORT

January 16, 1992

1. ARO Proposal Number: 29276-GS

2. Period Covered by the Report: July 15, 1991 to November 14, 1991

3. Title of Proposal: "Monte Carlo Simulations of Random Rough Surface Scattering with Finite Element and Finite Difference Methods"

4. Contract/Grant Number: DAAL03-91-G-0217

5. Name of Institution: University of Washington

6. Authors of Report: Leung Tsang and Chi Hou Chan

7. Scientific Personnel Supported By this Project:
   Leung Tsang, Principal Investigator
   Chi Hou Chan, Co-Principal Investigator
   Charles Mandt, Research Assistant

Summary of the Research Findings

The earlier formulation of Monte Carlo simulations of scattering of waves by perfectly conducting random rough surfaces based on the finite-element method and periodic boundary condition is extended to investigate scattering from one-dimensional random rough gold surfaces at optical frequencies. In this report, two cases are investigated. For Case 1, the random surfaces have a correlation length of 3.099λ and a root-mean-square height of 1.6927λ, and the refractive index of $0.312 + i7.93$ is used. For Case 2, these numbers are 1.0525λ, 0.5749λ, $1.958 + i20.7$, respectively. Both TE and TM plane-wave incidences at 0^0, 10^0, and 30^0 are considered. The finite conducting surfaces are modeled as lossy dielectric rough surfaces. To reduce the computational domain, for the TE case, we insert a perfect electric conducting (PEC) wall which has the same rough surface profile at a few skin depths below the air-dielectric interface. Similarly, for the TM case, a perfect magnetic conducting (PMC) wall is used.

In our formulation, the scattered field slightly above a reference plane at a small distance (0.5λ) above the maximum height of the rough surface is expanded in terms of Floquet modes. The region bounded by this reference plane at the top, the conducting plane at the bottom, and the periodic boundary condition on the two sides is calculated using the finite elements with the field at the reference plane being specified as cosine or sine functions. We call these solutions finite-element modes. There is no one-to-one correspondence between the FEM modes and the Floquet modes. In fact, each of the FEM modal solutions in the region very close to the rough surface incorporates all the propagating modes and a large number of evanescent modes. Most of these evanescent modes, however, decay to zero at the reference plane. For each of the finite-element modes, we solve a Helmholtz equation in which we use a discretization of 6 nodes per linear wavelength for all the calculations reported here. The FEM calculation is very efficient with the use of a sparse matrix solver. The amplitudes of the Floquet modes are calculated by matching the field and its normal derivative represented by the Floquet modes

and linear combinations of FEM modes on the two sides of the reference plane. The fast Fourier transform (FFT) algorithm has been used in the process to improve numerical efficiency. Extensive numerical experiments show that only four to six evanescent modes are needed. The maximum error in the power conservation is less than 1 % when the lossy medium is replaced by a lossless one. There are two propagating Floquet modes for each wavelength of the surface length. Therefore, a full matrix equation of the order of 2 [*integer* (L / λ)] + N_E + 1 needs to be solved, where N_E is the number of evanescent modes and L is the surface length. In the calculation of surface length of 50λ, we have used 101 propagating modes and 4 evanescent modes, a total of 105 Floquet modes. The same number of FEM modes are used. In contrast, for the spectral domain extended boundary method in which the field is expanded right on the rough surface, as many evanescent modes as propagating ones are often required for the large surface height considered in this study. On the other hand, a full matrix of the order 1000 x 1000 is required for the integral equation method for this two-medium problem when a discretization of 10 per linear wavelength is used for the rough surfaces under consideration.

In the numerical results to follow we present the radar cross sections of the rough surface for both TE and TM incidences at 0^0, 10^0, and 30^0 at the wavelengths of 1.152 μm (Case 1) and 3.392 μm (Case 2). To investigate the effect of the surface length L to the radar cross section, two surface lengths, namely, $L = 30\lambda$ and 50λ are used for Case 2 with the TM incidence at 30^0. Figure 1 shows that the RCS exhibits two peaks, one at the backscattering direction and the other at the specular direction, when the surface length is small. In Figure 2, however, the specular peak is suppressed while the backscattering is enhanced when we increase the surface length to 50λ. For this two-medium problem, due to limited computer resources, we chose all our surface lengths to be 50λ. Figures 3 to 14 show the RCSs for all the 12 cases. We summarize our findings as follows: (1) both the TE and TM incidences show backscattering enhancement at all three incident angles; (2) it is also found that while the TE and TM responses are very similar in Case 1, TE incidence yields stronger backscattering enhancement in Case 2, in contrast to the scattering from surfaces with small roughnesses where backscattering enhancement is observed only for the TM waves; (3) of all the numerical simulations, the lossy surfaces absorb more power for the TM incidences than that of the TE; and (4) the absorption rate decreases with the incident angles.

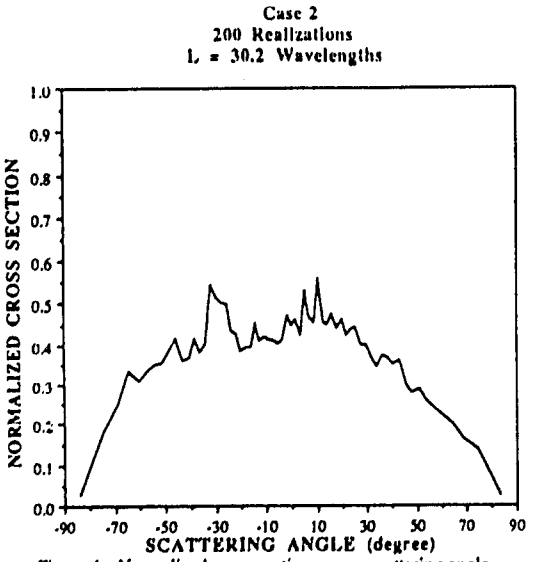

Figure 1. Normalized cross section versus scattering angle. TM incidence at 30 degree.

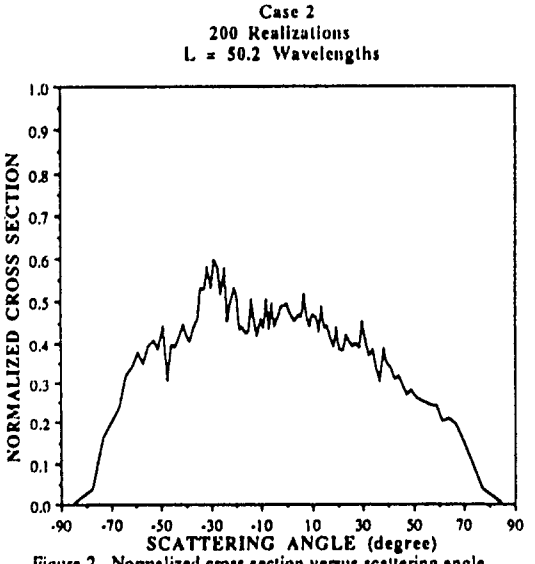

Figure 2. Normalized cross section versus scattering angle. TM incidence at 30 degree.

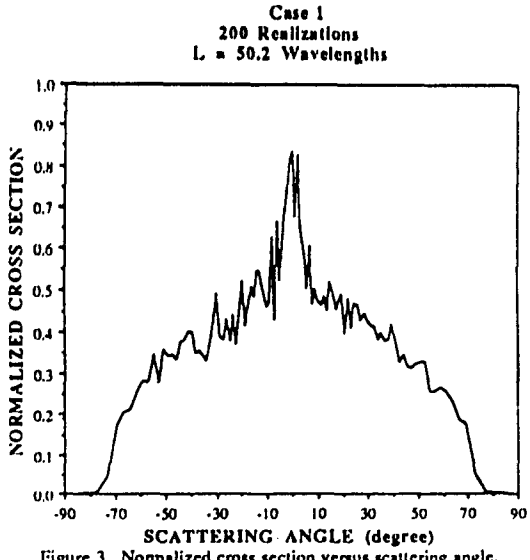

Figure 3. Normalized cross section versus scattering angle. TE incidence at 0 degree.

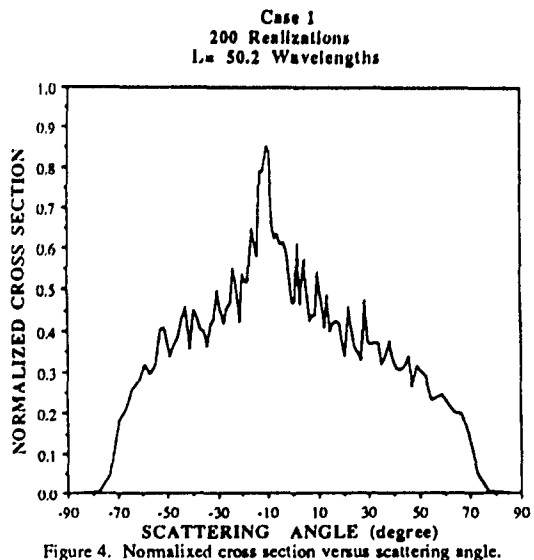

Figure 4. Normalized cross section versus scattering angle. TE incidence at 10 degree.

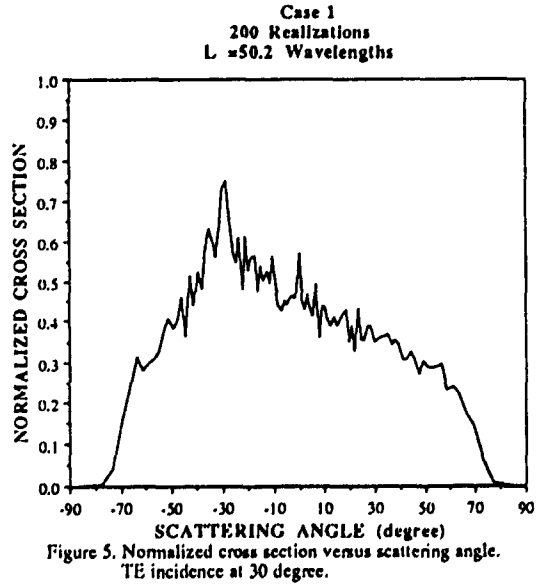

Figure 5. Normalized cross section versus scattering angle. TE incidence at 30 degree.

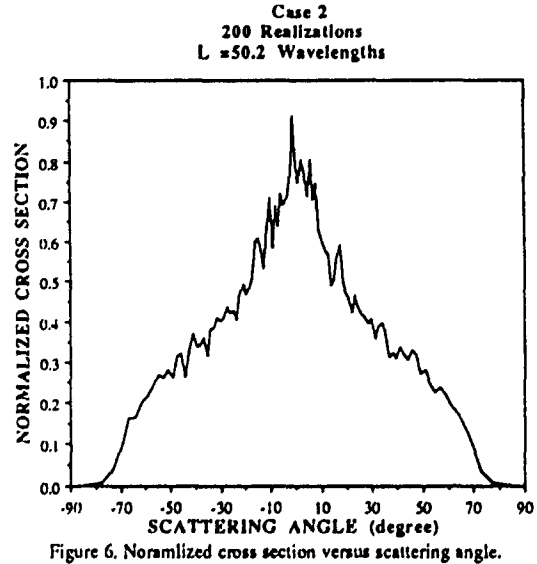

Figure 6. Normalized cross section versus scattering angle. TE incidence at 0 degree.

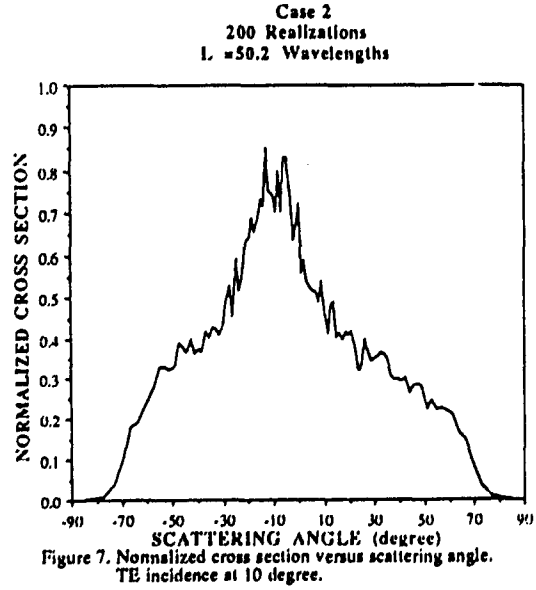

Figure 7. Normalized cross section versus scattering angle. TE incidence at 10 degree.

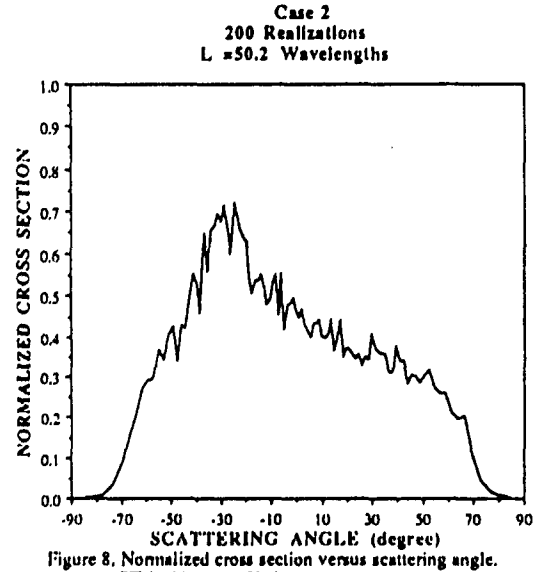

Figure 8. Normalized cross section versus scattering angle. TE incidence at 30 degree.

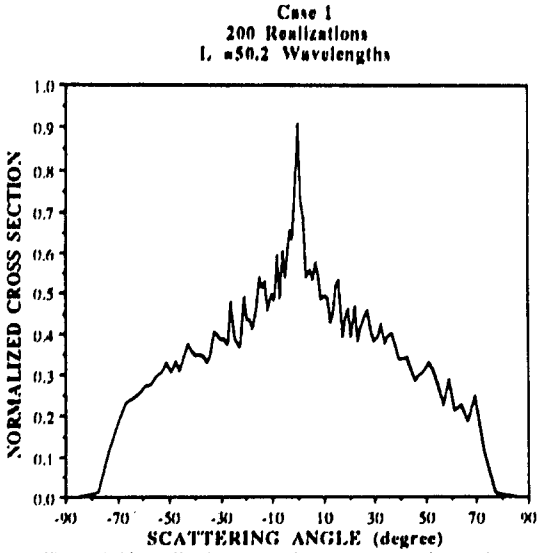

Figure 9. Normalized cross section versus scattering angle. TM incidence at 0 degree.

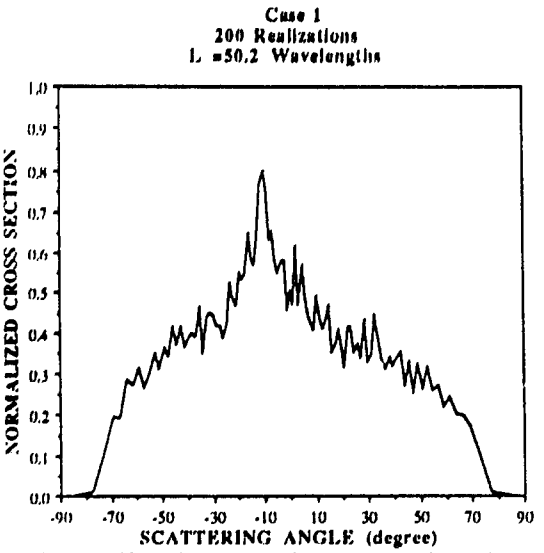

Figure 10. Normalized cross section versus scattering angle. TM incidence at 10 degree.

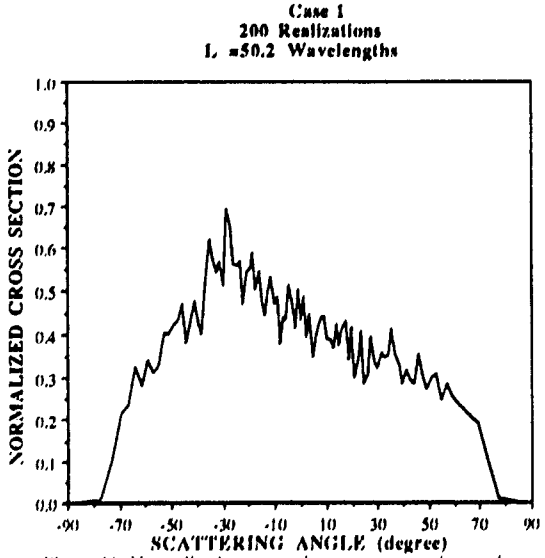

Figure 11. Normalized cross section versus scattering angle. TM incidence at 30 degree.

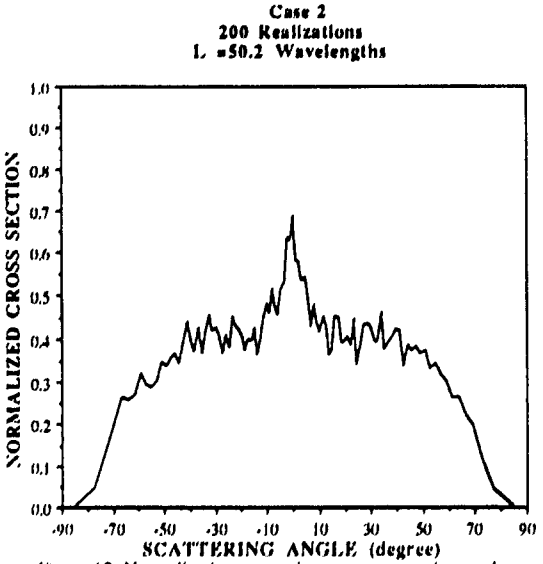

Figure 12. Normalized cross section versus scattering angle. TM incidence at 0 degree.

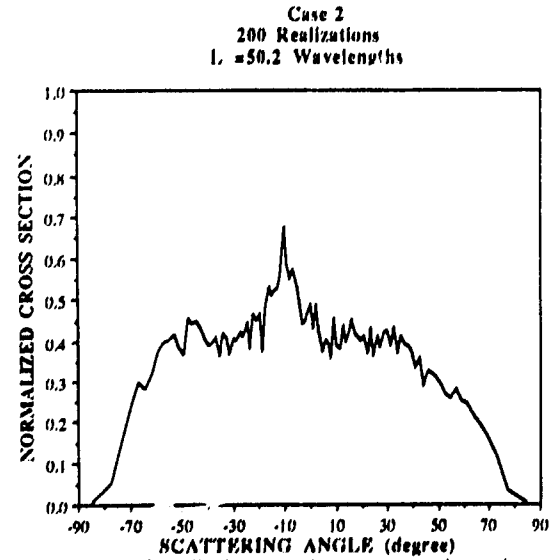

Figure13. Normalized cross section versus scattering angle. TM incidence at 10 degree.

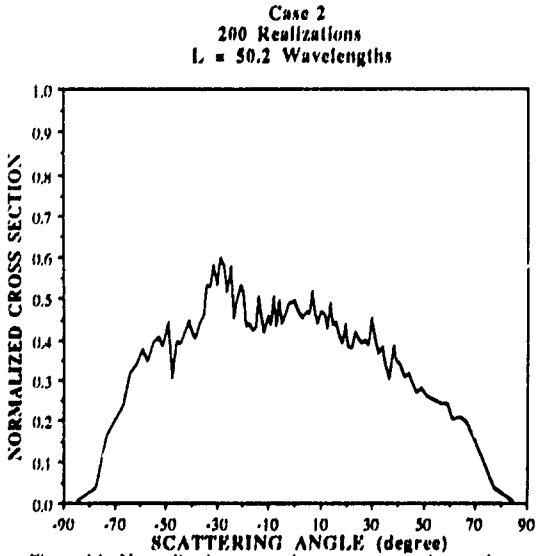

Figure 14. Normalized cross section versus scattering angle. TM incidence at 30 degree.